79-GT-64

Printed in U.S.A.

an ASME publication

$3.00 PER COPY
$1.50 TO ASME MEMBERS

Investigation of the Heat Transfer in Cylindrical Receiver Configurations with Inner Tubes

K. BAMMERT

Professor

R. KRAPP

Research Assistant

P. SEIFERT

Research Assistant

Institute for Turbomachinery and Gasdynamics,
University of Hannover,
Hannover, Germany

The design of a receiver for a closed-cycle gas turbine with air as the working medium is discussed. The emphasis of the investigations is layed upon the optimization of heat transfer to the working medium. The irradiation pattern along the tubes and the effects of the working-medium pressure, the pressure loss and the tube cage geometry are considered.

Contributed by the Gas Turbine Division of The American Society of Mechanical Engineers for presentation at the Gas Turbine Conference & Exhibit & Solar Energy Conference, San Diego, Calif., March 12-15, 1979. Manuscript received at ASME Headquarters December 18, 1978.

Copies will be available until December 1, 1979.

THE AMERICAN SOCIETY OF MECHANICAL ENGINEERS, UNITED ENGINEERING CENTER, 345 EAST 47th STREET, NEW YORK, N.Y. 10017

Investigation of the Heat Transfer in Cylindrical Receiver Configurations with Inner Tubes

K. BAMMERT **R. KRAPP** **P. SEIFERT**

ABSTRACT

The design of a receiver for a closed-cycle gas turbine with air as the working medium is discussed.

The emphasis of the investigations is layed upon the optimization of heat transfer to the working medium. The irradiation pattern along the tubes and the effects of the working-medium pressure, the pressure loss and the tube cage geometry are considered.

INTRODUCTION

A by human standards inexhaustable source of energy is provided by the sun. For the thermal conversion of solar energy into mechanical and electrical energy there are two possibilities. For smaller outputs the solar farm concept can be considered. Here the working medium is heated to about 350 ^{o}C in concentrating collectors connected in parallel. Problems arise here when designing turbo machines with small power ratings and small volume flow. Because of the low upper process temperature only low efficiencies are possible. If the solar radiation is concentrated by means of numerous heliostats onto a receiver in which the working medium is heated up, very high upper process temperatures and hence good efficiencies can be achieved. The receiver of such plants is mounted on a tower (Solar Tower Plants). High upper process temperatures can only be utilized by gas turbines. However, because of the higher costs this method is only economical in the case of large outputs. Problems arise here with the design of the receiver; these are due to the heat-transfer properties of the gaseous working medium and the high concentration of the solar radiation.

The closed-cycle gas turbine offers advantages in the utilization of solar energy which facilitate the design of the receiver. These plants allow a free choice of the working medium and the process pressure in the receiver, whereby the heat transfer in the receiver can be favorably effected.

The development of the closed-cycle gas turbine has been fully consolidated as regards layout, design, manufacture and operation. Five of these plants with air as the working medium have already been running for a total of more than 500,000 hours. Since 1974, the Oberhausen helium turbine has been providing valuable experience in the operation of such plants with helium as the working medium. Blast-furnace gas, mine gas, coal, oil, coke-oven gas and mixtures thereof are used as primary energy (1)[1]. In the heaters of closed-cycle air turbine plants the heat is transferred to the working medium in a radiation part and a convection part. The experience gained in the construction of these radiation parts will be utilized in the following paper for the design of a receiver for a 20-MW closed-cycle plant with air as the working medium. The aim is the optimization of the heat transfer to the working agent.

---

1 Numbers in parentheses designate References at end of paper.

DESCRIPTION OF THE CLOSED-CYCLE AIR TURBINE PLANT

Fig. 1 shows the scheme of circuit of the reference plant. Air is sucked in by the LP compressor a, recooled in the intercooler b, and compressed to the highest process pressure by the HP compressor c. In the recuperative heat exchanger d the working medium then absorbs the usable heat of the turbine exhaust gas before being heated up in the receiver e to the highest process temperature. After expansion in the turbine f, the air flows through the heat exchanger d where it gives off heat, and is cooled down in the precooler g to the LP compressor inlet temperature.

The design data of the plant are compiled in Table 1. The compressor inlet temperature was chosen as 50 °C. This value seems to be attainable with dry cooling and at an ambient temperature of approx. 40 °C. The upper process temperature was specified as 800 °C. With modern technology this temperature is achievable with metallic materials. The turbine inlet pressure was fixed at 4.4 MPa, and the other design data were based on air turbine plants already built. The thermodynamic optimization of the cycle resulted in an expansion ratio of 3.0 for the turbine. The efficiency at terminals is the ratio of the output at the terminals of the alternator and the heat absorbed by the working medium in the receiver. It is 38.3 %. At an output of 20 MW the turbine mass flow is 172 kg/s. Table 2 shows the influence of varied design parameters on the efficiency η at terminals.

For the plant described above the receiver was designed which has to transfer 52.5 MW of heat at a working-medium inlet temperature of 529.5 °C. Its relative total pressure loss is 4.9 % and is included in sum of total pressure losses of 12 %. The relative total pressure loss is defined

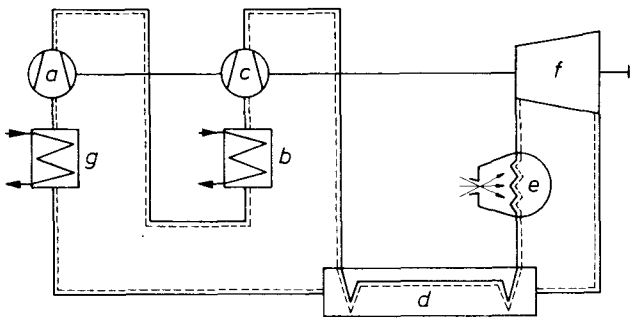

Fig. 1 Scheme of circuit of a solar tower plant

a LP compressor
b intercooler
c HP compressor
d recuperator
e receiver
f turbine
g precooler

Table 1 Layout parameters of a solar tower power plant with closed-cycle gas turbine

working fluid	air
output at terminals	20 MW
turbine inlet temperature	800 °C
number of intercoolings	1
turbine inlet pressure	4.4 MPa
pressure ratio of expansion	3.0
isentropic turbine efficiency	90.0 %
cooling coefficient	1 %
compressor inlet temperature	50 °C
pressure ratio of compression	3.35
isentropic compressor efficiencies (LP/HP)	86.0/85.0 %
temperature difference of recuperator	30 °C
efficiency of heat exchange	92.6 %
recuperator inlet temperature (cold)	122.8 °C
recuperator inlet temperature (hot)	559.5 °C
receiver inlet temperature	529.5 °C
sum of relative pressure losses	12 %
mechanical efficiency	99.7 %
gear efficiency	98.5 %
alternator efficiency	98.0 %
net efficiency	38.3 %
turbine mass flow	172.01 kg/s
volume flow at turbine inlet	$43.75 \cdot 10^3$ m³/h
volume flow at LP compressor inlet	$41.21 \cdot 10^3$ m³/h
volume flow at HP compressor inlet	$22.62 \cdot 10^3$ m³/h

Table 2 Influence of varied layout parameters on the net efficiency

varied parameter x	Δx	$\Delta\eta$ (additional percentage)
turbine inlet temperature	± 10 K	± 0.47
compressor inlet temperature	± 10 K	∓ 1.45
isentropic turbine efficiency	± 1 %	± 0.57
isentropic compressor efficiency	± 1 %	± 0.54
sum of the relative pressure losses	± 2 %	∓ 0.84
temperature difference of recuperator	± 10 K	∓ 1.32
cooling coefficient	± 1 %	∓ 0.83

as the pressure loss of the cycle component under observation, referred to its total pressure at the inlet. The relative total pressure loss of the complete plant is the sum of the individual relative total pressure losses.

CONCEPT OF RECEIVER DESIGN

In the receiver of a solar tower plant with gas turbine heat must be transmitted to a gaseous medium by radiation. The same applies to the radiation parts of fossil-fired heaters. For the calculation of such radiation parts there exist several methods (2, 3, 4) which are based on extensive measurements (5, 6, 7, 8, 9, 10).

In order to use this knowledge, the configuration of the receiver must be similar to that of the radiation parts of conventionally fired heaters. For this reason a cylindrical or polygonal receiver design is postulated. Fig. 2 shows the basic configuration of a cylindrical receiver. The working medium enters the inlet header a, flows

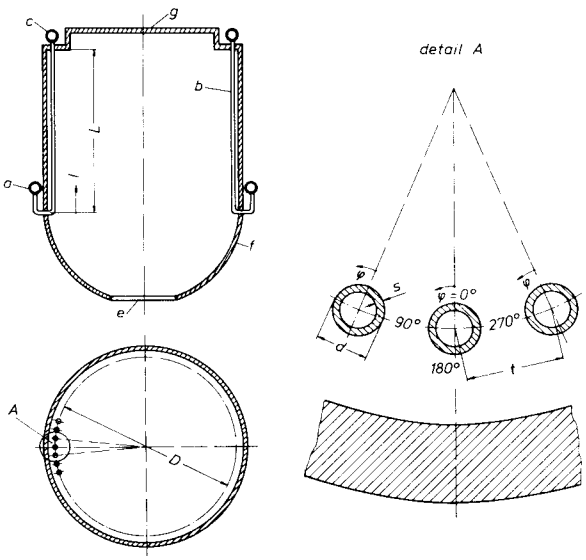

Fig. 2 Diagrammatic sketch of receiver configuration

a inlet header
b tubes
c outlet header
d diameter of turbes
e aperture
f reflective part of the receiver
g ceiling
l current length irratiated
s wall thickness
t spacing
D pitch diameter
L total irradiation length
φ segment angle

through the tubes b situated in front of the inner wall of the receiver, and leaves the receiver through the outlet header c. The total tube irradiation length is shown as L and the current length irradiated as l. The tubes have an outer diameter d and are arranged with a spacing t on a pitch diameter D.

In order to be able to describe the temperature pattern and the pattern of irradiation over the tube circumference, a segment angle φ is introduced for each tube. The zero point of this segment angle in each case is directed towards the receiver axis and marks the point of highest irradiation at the tube circumference.

It is assumed that the radiation caught by the reflectors will enter the receiver through an aperture e. Inside the receiver the radiation at first encounters a reflecting wall f which has the task of reducing the intensity of the radiation to which the tubes are subjected (11). The intensity pattern over the tube length L can be influenced by the shape of this part of the receiver and if necessary of the ceiling g. Part of this reflected radiation acts directly on the tubes and is largely absorbed by them. The remaining radiation acts on the receiver wall situated behind the tubes. If this wall is thermally insulated against the environment then the collected radiation is reradiated again mainly in the form of thermal radiation and largely absorbed by the tubes carrying the working medium. The energy not absorbed by the tubes leaves the receiver through the aperture and is lost for the process.

Since the admissible irradiation intensity inside the receiver is limited by the heat transfer to the medium, one must look for ways of improving this heat transfer.

The following investigations deal exclusively with the heat transfer to the working medium. As will be shown later, the irradiation pattern along the tubes has a major effect on this heat transfer. It is assumed that this pattern can be influenced by the configuration of the reflecting components f and g of the receiver. To optimize the heat transfer, the most effective way of distributing the radiation must first of all be found.

If the heat to be transferred, the working medium and its inlet and outlet temperatures are fixed, then the heat transfer is also dependent on

- the maximum controllable tube wall temperature,
- the tube diameter, d,
- the spacing ratio, t/d,
- the working-medium pressure, and
- the max. admissible relative total pressure loss.

The tubed part of the receiver of the above reference plant was investigated with regard to these variables. The calculation methods for the radiation parts of conventionally fired heaters were used and it was assumed that the radiation entering the receiver is distributed axisymmetrically over the tubed surface of the receiver.

PATTERN OF THE ABSORBED RADIATION INTENSITY

At a constant heat transfer coefficient between inner tube wall and working medium, the amount of heat transferred per unit of surface area is governed by the temperature difference between inner tube wall and working medium. Therefore this temperature difference should be as great as possible. Since the heat has to pass through the tube wall, the outer temperature of the tube as a function of the thermal conductivity of the tube material is higher than the temperature of the inner wall. The strength of the tubes is governed by the maximum temperature occurring, i.e. the outer tube wall temperature. If one succeeds in raising this temperature over the entire length of the tube to the maximum admissible value, then the temperature difference between inner tube wall and the working medium over the entire length of the tube likewise increases to the maximum possible value. The local tube wall temperature is determined to a decisive degree by the pattern of the irradiation absorbed by the tubes. This absorbed local irradiation, referred to the unit of surface area, is hereinafter called "heat flux". If one integrates the heat flux over the entire surface of all tubes then one obtains the transferred heat.

When designing a receiver that heating surface has to be determined which will transfer the required heat and with which the

maximum admissible tube wall temperature will not be exceeded. "Heating surface" here means the sum of the tube surfaces. Furthermore, the length and number of tubes at a given tube diameter must be fixed such that the admissible relative total pressure loss is not exceeded.

In order to match all the design conditions, at the start of the calculation only the pattern of the heat flux is specified and not the local absolute values. The heating surface and the absolute values of the heat flux over the length and circumference of the tubes are calculated.

For the receiver of the 20-MW plant the pattern of the heat flux along the tubes was varied. The chosen tube material was Incoloy 807, which permits tube wall temperatures of up to 860 °C. For the design case shown in Table 1, Fig. 3 shows the influence of the heat flux pattern on the distributions of the working-medium temperature and of the maximum tube wall temperature. A spacing ratio t/d = 2.3 and a tube diameter d = 40 mm were assumed. The maximum tube wall temperature occurs at a segment angle $\varphi = 0^{\circ}$ (cf. Fig. 2).

First of all a constant heat flux pattern over the tube length was specified. In the left half of Fig. 3 the calculated absolute values of the heat flux are plotted against the relative tube length l/L (curve a, top), and the associated curves for tube wall temperature b and working-medium temperature c are shown in the bottom part. One can see that the temperature potential of the tube material is not utilized, since the admissible tube wall temperature of 860 °C only occurs at the outlet of the irradiated part. On account of the constant heat flux the two curves run parallel to each other.

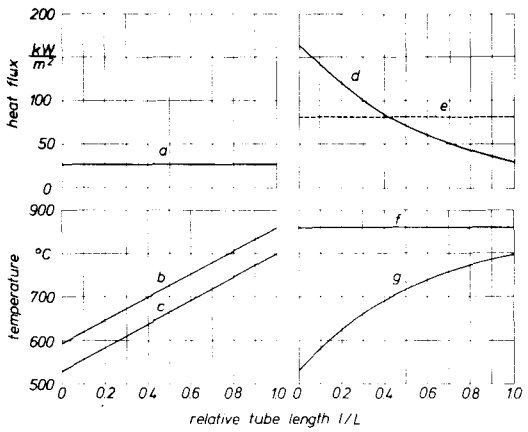

Fig. 3 Influence of irradiation on heat flux and temperature

a heat flux for constant irradiation
b maximum tube temperature for constant irradiation
c air temperature for constant irradiation
d heat flux for optimized irradition
e mean heat flux for optimized irradiation
f maximum tube temperature for optimized irradiation
g air temperature for optimized irradiation

The required heating surface (635 tubes) is approx. 1,960 m^2. The irradiated tube length is 24.6 m and the pitch diameter D is 18.6 m. In the case of constant irradiation over the length of the tubes the mean heat flux assumes a value of 26.9 kW/m^2. The mean heat flux is the quotient obtained from transferred heat and heating surface.

The heat transferred per unit surface can be considerably increased if the maximum admissible tube wall temperature is attained over the entire length of the tubes. Starting with constant irradiation, the pattern of the heat flux along the tubes was improved until a constant tube wall temperature of 860 °C for the segment angle $\varphi = 0^{\circ}$ was reached. The irradiation thus optimized (curve d) is shown in the upper right portion of Fig. 3. One can see that the mean heat flux e with a value of 81.7 kW/m^2 is about 3 times higher than at constant irradiation. The maximum heat flux occurs at the working-medium inlet and is approx. 166 kW/m^2. Here the difference between the tube wall temperature f and the working-medium temperature g has its greatest value, too. As the temperature difference decreases, the transferable heat also decreases.

For this optimized irradiation pattern the heating surface is 646 m^2. 464 tubes with a length of L = 11.1 m are required, arranged on a pitch circle with a diameter of D = 13.6 m.

The optimum heat flux pattern thus calculated was made non-dimensional with the mean heat flux and used as a basis for all further calculations. As a result, in all the following variations a constant tube wall temperature of 860 °C over the whole length of the tube is achieved for the segment angle $\varphi = 0^{\circ}$.

INFLUENCE OF THE TUBE SPACING RATIO AND OF THE TUBE OUTER DIAMETER

The tube spacing ratio influences the proportion of radiation acting on the inner receiver wall. At a spacing ratio of t/d = 1 the inner wall does not receive any radiation, so the tube surface in the segment angle range $90^{\circ} < \varphi < 270^{\circ}$ (see Fig. 2) does not absorb any radiation energy. However, this range participates in the heat transfer to the working medium because of the thermal conduction occurring in the tube wall in circumferential direction. In the irradiated range of the tube surface between $\varphi = 270^{\circ}$ and $\varphi = 90^{\circ}$ the inner tube wall temperature is higher than on the opposite side. Heat is therefore additionally transferred by radiation to the inner tube wall for the segment angle range $90^{\circ} < \varphi < 270^{\circ}$. The working medium absorbs the heat from the inner tube wall by convection.

As the spacing ratio increases, the inner receiver wall receives more and more radiation energy which is reradiated again, so the portion of tube surface facing the inner receiver wall also absorbs heat energy.

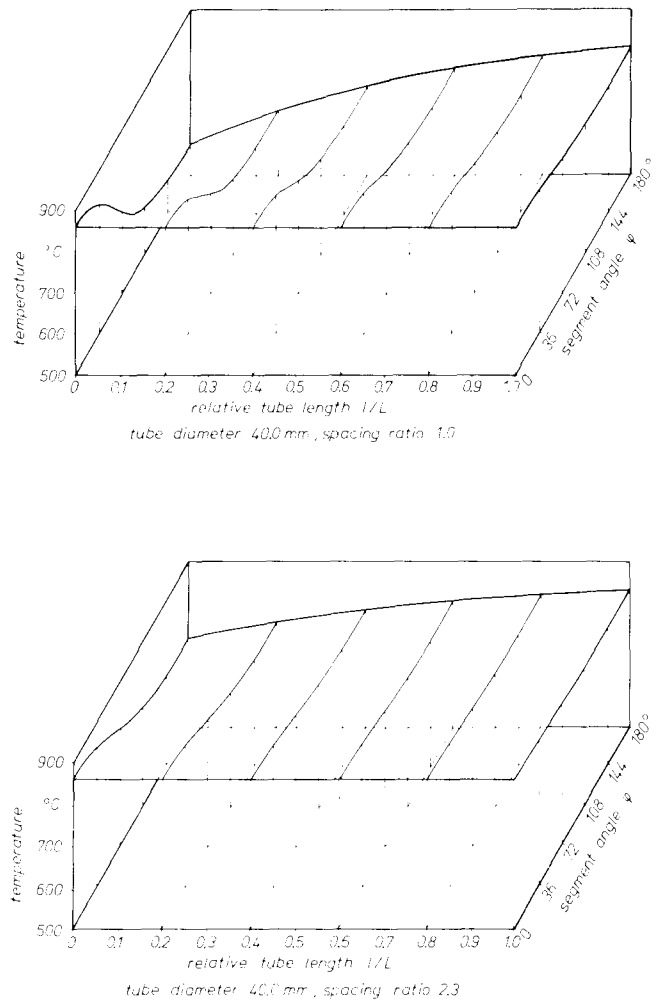

Fig. 4 Temperature distribution on tube surface

The higher the chosen spacing ratio, the higher this proportion of the total energy absorbed by the tube becomes, and the temperatures on the tube surface approach the maximum admissible tube wall temperature for very high spacing ratios.

Fig. 4 shows the temperature distribution on the tube surface along the relative tube length 1/L and the tube segment angle φ for the spacing ratios t/d = 1.0 (top) and t/d = 2.3 (bottom). The tube diameter is in both cases d = 40 mm. The temperatures are only given for the range between $\varphi = 0^{\circ}$ and $\varphi = 180^{\circ}$, since the temperature pattern is symmetrical with the axis connecting the angles $\varphi = 0^{\circ}$ and $\varphi = 180^{\circ}$.

One can clearly recognize that in both cases the tube wall temperature over the entire length of the tube for the segment angle $\varphi = 0^{\circ}$ reaches the max. admissible value of 860 °C. As the segment angle increases, the temperature gradient along the tubes also rises. The temperature pattern at a spacing ratio t/d = 2.3 is much more uniform. The lowest tube wall temperature occurs at 1/L = 0 and $\varphi = 180^{\circ}$. At a spacing ratio of t/d = 1.0 it is 577 °C, being much lower than the value of 776 °C at t/d = 2.3.

At constant working-medium pressure the tube wall thickness increases with the outer diameter. This reduces the transfer of heat through the tube wall, i.e. at constant outer tube wall temperature less heat per unit of surface area is transferred to the working medium.

As the tube circumenference increases, the thermal conduction in circumferential direction decreases. This leads to greater temperature differences on the tube periphery. At constant maximum tube wall temperature the mean temperature difference between inner tube wall and working medium therefore decreases. This also reduces the heat transfer rate to the working medium.

For the distribution of the radiation in the receiver the ratio of the irradiated tube length to the inner diameter of the receiver is of great importance. The inner diameter of the receiver is largely governed by the pitch diameter. Favourable conditions for irradiation are to be expected at values for L/D of between 0.8 and 1.2.

For the outer tube diameters 30.0 mm, 40.0 mm and 50.0 mm the spacing ratio t/d was varied between 1.0 and 4.0. The thermodynamic data correspond to the cycle design data of Table 1. For the receiver a spacing ratio t/d = 2.3 and a outer tube diameter d = 40.0 mm were chosen. This choice is justified as follows:

In Fig. 5 the mean heat flux (left) and the ratio of the irradiated tube length L to the pitch diameter D (right) for the three tube diameters under observation are plotted against the spacing ratio. At constant tube diameter the mean heat flux increases as the spacing ratio rises, since the tube surface is irradiated more evenly. As already explained, the heat flux decreases as the tube diameter increases.

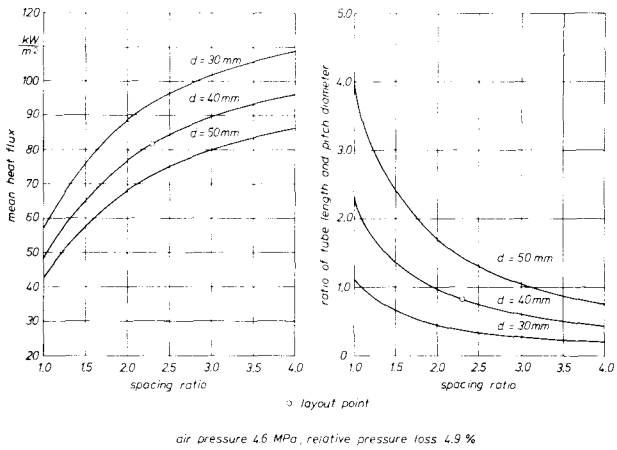

Fig. 5 Mean heat flux and the ratio of tube length and pitch diameter as a function of the spacing ratio

From the right-hand portion of Fig. 5 it can be seen that the ratio of the irradiated tube length L to the pitch diameter D decreases as the spacing ratio increases. Because of the increase in the mean heat flux the required heating surface becomes smaller. Since the tube length decreases more sharply than the number of tubes, the result is the curve shown.

At constant spacing ratio the quotient from L/D increases with the diameter. This is basically caused by the fact that at constant pressure loss the required number of tubes decreases as the tube diameter increases.

If one keeps to the aforementioned limits for L/D from 0.8 to 1.2, then for a tube diameter of 30.0 mm only spacing ratios between 1.0 and 1.3 can be considered. The mean heat fluxes thus achievable are between 57.0 and 68.5 kW/m^2. At a diameter of 40 mm under these circumstances the spacing ratio can be between 1.68 and 2.36. The associated mean heat fluxes are between 69.5 and 82.5 kW/m^2. For the entire range these values are higher than those for d = 30.0 mm. For the tube diameter d = 50.0 mm the spacing ratios are between 2.65 and 3.82. The associated heat fluxes are between 75.5 and 85.5 kW/m^2. At spacing ratios of more than 3.32, higher mean heat fluxes can be achieved here than with an outer diameter of 40.0 mm. However, with a spacing ratio of 3.32 and a tube diameter of d = 50.0 mm the irradiated tube length is 14.23 m and the pitch diameter 15.16 m. The volume calculated with these values is approx. 2,570 m^3, and is by 60 % greater than in the case of the chosen design with a spacing ratio of 2.3 and a tube diameter of 40.0 mm. This is why a tube diameter of 50.0 mm was not considered.

INFLUENCE OF THE WORKING-MEDIUM PRESSURE

If the working-medium temperature and the pressure loss are kept constant, then the Reynold's number increases as the pressure rises. This results in better heat transfer on the inside of the tubes. However, at constant outer tube diameter the wall thickness increases, which means a reduced heat transfer rate through the tubes.

In Fig. 6 for the chosen tube diameter of 40.0 mm and the spacing ratio 2.3, the mean heat flux is plotted against the receiver inlet pressure. As the pressure increases, the heat flux initially rises sharply, since the improved heat transfer to the working medium predominates over the influence of the increased tube wall thickness. Between 4.0 and 4.9 MPa the greatest heat fluxes are achieved. In this range the curve is flat and attains values of around 82.5 kW/m^2. At pressures above 4.9 MPa the influence of the tube wall thickness predominates, so the mean heat flux falls off again.

For the chosen turbine inlet pressure of 4.40 MPa and a relative total pressure loss of ε = 4.9 % for the receiver, the resulting receiver inlet pressure is 4.61 MPa. This pressure lies in the optimum range of

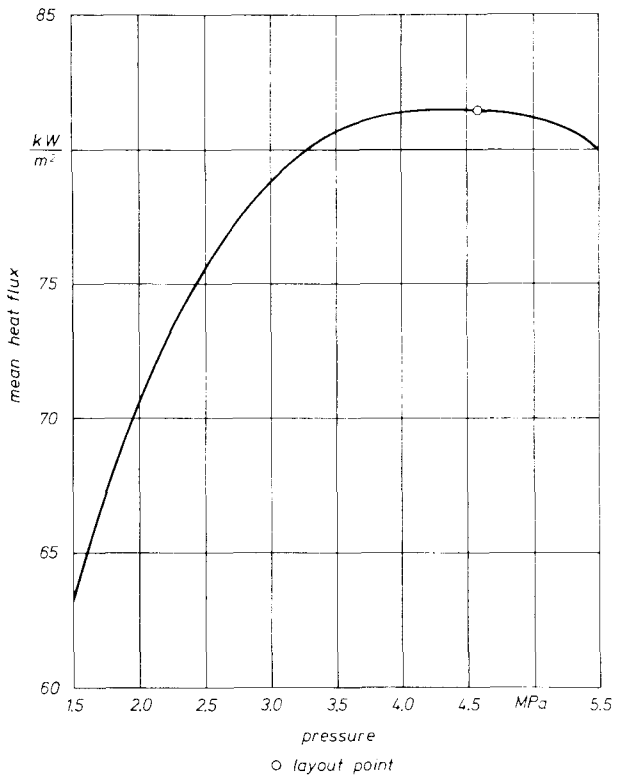

tube diameter 40.0 mm, spacing ratio 2.3, relative pressure loss 4.9%

Fig. 6 Mean heat flux as a function of receiver inlet pressure

the curve and is specially marked. At a tube outer diameter of 40.0 mm the tube wall thickness is 7.3 mm.

INFLUENCE OF THE RELATIVE TOTAL PRESSURE LOSS

If one increases the working-medium velocity, then the heat transfer on the inside of the tubes is likewise improved. However, a higher pressure loss must be accepted in this case, resulting in a lower efficiency of the plant. If the output at the terminals is kept constant, then the heat to be transferred is increased.

At the turbine pressure ratio of expansion of 3.0 given in Table 1 the relative total pressure loss of the receiver was varied. In Fig. 7 the mean heat flux a and the heating surface b, each referred to the corresponding design value of 81.7 kW/m^2 and 646.0 m^2, respectively, are plotted against the difference between the relative pressure loss and the design pressure loss of 4.9 %. The second absciss shows the difference between the efficiency and the design efficiency of 38.3 %.

The relative mean heat flux increases with rising pressure loss since the heat transfer on the inside of the tube is improved. For very high pressure losses the curve runs towards a limit value. This limit value is governed by the thermal conductivity of the tube material.

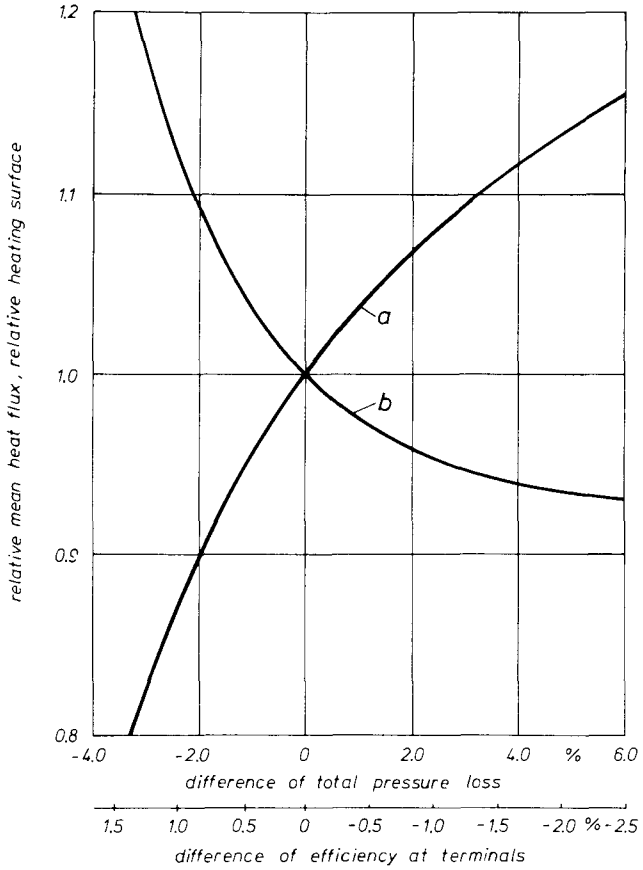

Fig. 7 Influence of total pressure loss on the receiver design

a relative mean heat flux
b relative heating surface

As the pressure loss increases, the relative heating surface decreases less sharply than the mean heat flux increases. This is due to the fact that as the pressure loss rises, the efficiency is reduced, so that at constant output at the terminals more heat must be transferred to the working medium.

SUMMARY

A receiver was designed for a solar tower plant with closed-cycle gas turbine. The output at the terminals of the plant, which uses air as the working medium, is 20 MW. At an efficiency of 38.3 %, 52.2 MW of heat must be transferred in the receiver to the working medium.

For the design of the receiver the influence of the irradiation pattern, spacing ratio, outer tube diameter and receiver inlet pressure were investigated with regard to the heat transfer. An irradiation curve was stated which will permit optimum utilization of the tube material and enable a maximum heat flux of 166 kW/m^2 and a mean heat flux of 81.7 kW/m^2 to be achieved. Small tube diameters and high spacing ratios favour heat absorption in the receiver. However, a compromise must be found between the required heating surface and the size of the receiver. The receiver design is furthermore influenced by the receiver inlet pressure. For the receiver under investigation the optimum pressure range was shown to be between 4.0 and 4.9 MPa. The design data of the receiver are compiled in Table 3.

For the designed receiver a variation of the relative total pressure loss was carried out. As the pressure loss increases, the required heating surface decreases. However, the relative total pressure loss of the receiver must not be viewed in isolation, since it influences the efficiency of the complete plant.

Table 3 Layout parameters of the receiver

transferred heat	52.2 MW
mean heat flux to the air	81.7 kW/m^2
maximum heat flux to the air	166.0 kW/m^2
mass flow	172.01 kg/s
receiver inlet temperature	529.5 °C
receiver outlet temperature	800.0 °C
receiver inlet pressure	4.61 Mpa
pressure loss	4.9 %
maximum allowable tube temperature	860.0 °C
tube dimension	40 x 7.3 mm
length of irradiated tubes	11.1 m
pitch diameter	13.6 m
tube spacing ratio t/d	2.3
number of tubes	464
heating surface	646 m^2

REFERENCES

1 Bammert, K., and Groschup, G., "Status Report on Closed-Cycle Power Plants in the Federal Republic of Germany," Transactions of the ASME, Vol. 99, No. 1, 1977, pp. 37-46.

2 Bammert, K., and Sunkel, K., "Die wirtschaftliche Auslegung der Strahlungsheizflächen von Lufterhitzern für Heißluftturbinen," Mitteilungen der Vereinigung der Großkesselbetreiber (VGB), Vol. 97, 1965, pp. 266-279.

3 Bammert, K., and Nickel, E., "Design of Combustion Chambers of Heaters for Transmission of the Primary Heat of Closed-Cycle Gas Turbines," ASME Gas Turbine Conference, Zurich, Switzerland, 1966, ASME Paper No. 66-GT-CLC-1.

4 Bammert, K., Kläukens, H., and Nickel, E., "Die Wärmeaufnahme und die örtliche Einstrahlung von Brennkammern geschlossener Gasturbinen," VDI-Zeitschrift, Vol. 109, No. 7, 1967, pp. 297-302.

5 Bammert, K., and Rehwinkel, H., "Berechnung des Temperaturfeldes und der Wärmeübertragung in zylindrischen Brennkammern," Forschung im Ingenieur-Wesen, Vol. 40, No. 2, 1974, pp. 37-46 and No. 3, 1974, pp. 87-96.

6 Bammert, K., "Zur Entwicklung des kohlenstaubgefeuerten Lufterhitzers," VDI-Zeitschrift, Vol. 100, No. 20, 1958, pp. 841-850.

7 Bammert, K.,and Keller, C., "Meßergebnisse der ersten kohlenstaubgefeuerten Heißluftturbinenanlage für Stromerzeugung und Heizwärmelieferung," Brennstoff-Wärme-Kraft (BWK), Vol. 12, No. 2, 1960, pp. 62-64.

8 Bammert, K., Geissler, Th.,and Nickel, E., "Die Verfeuerung von Kohlenstaub in Gasturbinenanlagen mit geschlossenem Kreislauf," Brennstoff-Wärme-Kraft (BWK), Vol. 14, No. 11, 1962, pp. 537-545.

9 Bammert, K.,and Rehwinkel, H., "Measurements on a Blast-Furnace-Gas and Oil-Fired Combustion Chamber of a 17.25 MWe Closed-Cycle Gas Turbine Plant," ASME-Gas Turbine Conference, Brussels, Belgium, 1970, ASME-Paper No. 70-GT-70.

10 Bammert, K., Bohnenkamp, W.,and Rehwinkel, H., "Versuchsergebnisse der mit Gichtgas und Öl gefeuerten Heißluftturbinenanlage Gelsenkirchen," Stahl und Eisen, Vol. 91, No. 6, 1971, pp. 309-314.

11 Gintz, J.R., "Closed-Cycle, High-Temperature Central Receiver Concept for Solar Electric Power," Boeing Engineering and Construction, Interim Report EPRI ER-183, 1976.